5636 *Macromolecules* **2009**, *42*, 5636–5641
DOI: 10.1021/ma900198k

Macromolecules
ARTICLE

Elastomers with Reversible Nanoporosity

Piotr P. Szewczykowski,[†] Kenneth Andersen,[†,‡] Lars Schulte,[†,‡] Kell Mortensen,[§] Martin E. Vigild,*[,†,⊥] and Sokol Ndoni*[,‡]

[†]*Danish Polymer Centre, Department of Chemical and Biochemical Engineering, Technical University of Denmark, DK-2800 Kgs. Lyngby, Denmark,* [‡]*Department of Micro and Nanotechnology, Technical University of Denmark, DK-4000 Roskilde, Denmark, and* [§]*Biophysics Group, Department of Basic Sciences and Environment, University of Copenhagen, DK-1871 Frederiksberg C, Denmark.* [⊥]*Presently: Dean of Undergraduate Studies and Student Affairs, Technical University of Denmark.*

Received January 29, 2009; Revised Manuscript Received June 6, 2009

ABSTRACT: An elastomer was created via cross-linking a diene block of a polyisoprene−polydimethylsiloxane (PI−PDMS) block copolymer in the ordered state of hexagonal morphology, followed by the quantitative removal of the PDMS component. The elastomer material collapsed following etching of the PDMS and apparently showed no resulting nanoporosity or structure resembling the precursor morphology in contrast to similar polydiene-based nanoporous material. However, the collapsed elastomer displayed surprising properties when exposed to a solvent. In the gel state the material recovers the original nanostructure and displays liquid-filled cavities. Upon several cycles of swelling and drying the cavities open and close in a reversible fashion. When exposed to a nonsolvent, the material remains collapsed. This discriminating behavior of liquid-material interaction holds potential for the use of these materials in advanced separation or load-release systems.

Introduction

Smart polymeric materials attract major attention among researchers within applied as well as basic science.[1−5] Such materials are characterized by having predetermined responses to external stimuli, which for example can be electrical, mechanical, or chemical. Often the response takes the form of a change in shape or size, possibly induced by a phase transition. Polymeric actuators are prominent examples of such materials, where electrical energy results in mechanical motion.[6] A very simple stimulus is temperature change which is exploited in thermoresponsive systems by controlling a volume phase transition of the material.[7] Chemical stimuli which trigger a shift of physicochemical properties could be a change in pH, selective solubility of a solvent, or a change in salt concentrations. Especially diblock copolymers show structural changes when exposed to solvents that interact differently with the polymer blocks. This is the case for block copolymer-based micelles induced by using a specific solvent at a given temperature[8] or selective swelling of block copolymer melts which causes phase transitions and morphology changes.[9] However, these phenomena do not traditionally qualify block copolymers as smart materials, although there are examples of solvent-triggered stimuli responsive materials which are used to create smart surfaces based on forms of block copolymers.[10]

Nanoporous materials derived from block copolymers hold potential for many different nanotechnological applications[11,12] and are also candidate materials for smart applications. An obvious application of nanoporous block copolymer-based materials is in membrane technology. A smart membrane could for example be used in controlled or selective diffusion which depends on the nature of the feed liquid for the membrane. Such a membrane would offer exceptional characteristics in separation processes with the option of including a valve effect which could allow the membrane to be open or closed for filtration of a liquid.

In our previous work we have shown how polydiene-based diblock copolymers containing polydimethylsiloxane (PDMS) establish a fine and versatile platform for creating nanoporous materials. Opportunities are plentiful for combining synthesis to obtain nanostructured materials of different morphologies and chemical composition with various procedures to modify or functionalize the matrix material.[13−16] The nanoporous structures are crucially dependent on the nature and the mechanical strength of the matrix material. In the case of matrices that are not crystalline or glassy at room temperature (as is the case with polydienes), it is necessary to reinforce the matrix (for example, by cross-linking the polymer) in order to have a structure which remains stable after selective etching of the expendable block during the process of fabricating the nanoporous material. In an earlier report we have characterized a series of samples with relatively low degrees of cross-linking of the matrix domain and observed that the nanostructure and porosity apparently are not detectable by small-angle scattering measurements after finishing the fabrication procedure.[13] It is reasonable to describe these materials as *collapsed*, but it is unresolved what the characteristics, morphology, and physicochemical properties are for these materials, which all have been treated in such a way that the expendable component of the precursor diblock copolymer matrix was quantitatively removed.

The aim of the work presented here is to conduct a structural study of collapsed samples (of low degrees of matrix cross-linking), which in the dry state do not produce well-defined nanoporous material. This study is primarily based on small-angle neutron scattering (SANS) measurements. Of special interest is the effect of exposing the collapsed samples to specific liquids, namely a solvent and a nonsolvent to the matrix material. Transmission electron microscopy (TEM) and small-angle X-ray scattering (SAXS) were used to characterize the dry samples.

*Corresponding authors. E-mail: mev@kt.dtu.dk (M.E.V.); sokol.ndoni@nanotech.dtu.dk (S.N.).

 Published on Web 07/15/2009

Table 1. Characteristics of the Precursor Diblock Copolymer

precursor sample	$\langle M_n \rangle_{PI}$[a] [g/mol]	$\langle M_n \rangle_{total}$[b] [g/mol]	PDI_{total}[c]	w_{PDMS}[d]	f_{PDMS}[e]	morphology [SAXS]	T_{ODT} [°C]
ID33	10 530	14 200	1.1	0.26	0.26	HEX	225

[a] Number-average molecular weight of the polyisoprene block as obtained by ^{1}H NMR. [b] Number-average molecular weight of the diblock molecule obtained by SEC and ^{1}H NMR. [c] Polydispersity index obtained by SEC. [d] Mass fraction of PDMS determined by ^{1}H NMR. [e] Volume fraction of PDMS at 20 °C calculated from density values: $\rho_{PI} = 0.900$ g/cm^3 and $\rho_{PDMS} = 0.966$ g/cm^3.[20,21] The morphology was determined by small-angle X-ray scattering (SAXS), and the order−disorder temperature (T_{ODT}) was determined by rheology measurements.

From this study we will gain information on the structure and nature of the low degree cross-linked samples and test these collapsed materials for possible smart behavior.

Experimental Section

Material Preparation. *Block Copolymer Synthesis*. The PI−PDMS block copolymer was prepared by sequential "living" anionic polymerization under an inert argon atmosphere as described elsewhere.[17] Samples described in this article derive from the ID33 batch of polymerization. The capital letters represent the chemical structure of the block copolymer, where PI is indicated by letter "I" and the PDMS is indicated by letter "D". The number following the letters "ID" is the batch number. The volume fraction of PI was targeted at $w_{PI} = 0.74$ to give a block copolymer system with hexagonally distributed cylinders of PDMS in a matrix of PI. Data for the parent sample ID33 are summarized in Table 1.

Alignment of Hexagonal Structure. In order to get optimal insight into the structural properties, as determined by the SANS experiment, the morphologies of the samples were aligned into a simple texture by extruding the polymer melt. For this purpose an extrusion device with a rectangular die of cross section 1×10 mm and 20 mm in length was constructed. Approximately 6 g of polymer was dissolved in 60 mL of tetrahydrofuran (THF) and cast in a glass covered by aluminum foil at the bottom. After solvent evaporation the aluminum foil was rolled, placed in the extruder, and squeezed. This helped to avoid bubbles in the extruded polymer. The polymer was extruded onto microscopy cover glasses prior to the cross-linking procedure.

Cross-Linking. The samples were cross-linked by using dicumyl peroxide (bis(α,α-dimethylbenzyl) peroxide) (DCP) from Merck in a step-by-step procedure. For dosage of DCP we make reference to the total number (mole) of double bonds in the sample in question. For the first cross-linking step an amount of DCP was scaled off which equal 2 mol % relative to the moles of double bonds in the sample volume (i.e., mol DCP/mol double bonds = 0.02). The 2 mol % of DCP was placed directly on the sample surface inside a homemade stainless steel cap screw cylinder equipped with two valves. Nitrogen gas was run through the cylinder for few minutes, and then the cylinder was tightened and placed in a preheated oven at 140 °C for 2 h with a nitrogen atmosphere as an additional precaution.[18] After baking, the cylinder was rapidly cooled down, and the sample was placed in a vacuumed round-bottom flask at 130 °C for 1 h to get rid of any accumulation of byproduct. For subsequent cross-linking steps an amount equivalent of 6 mol % of DCP was used. This procedure was repeated 2−3 times to give samples ID33-x14 and ID33-x20, where "x" symbolizes the cross-linking and the numeral refers to the total amount of added DCP (in mol %).

Etching of PDMS. A solution of 1 M tetrabutylammonium fluoride (TBAF) in THF from Aldrich was used as cleaving reactant for removing the PDMS blocks. Five times molar excess of TBAF relative to the PDMS repeating unit was used to etch the cross-linked PI−PDMS samples. The reaction time was 24 h at room temperature. The samples were rinsed with THF and methanol prior to drying. Samples were code named by adding the suffix "e" for etching to the sample name; hence, the sample names become ID33-x14e and ID33-x20e.

Characterization Techniques. *Chromatography*. Size exclusion chromatography (SEC) in stabilized THF was used to determine the molar mass and molar mass distribution of the copolymer blocks. SEC equipment consisted of two mixed-D columns (Polymer Laboratories) and a triple detector setup (Viscotec) (right angle light scattering, viscometer, and differential refractometer).

Spectroscopy. The diblock copolymer average composition was determined by proton magnetic resonance spectroscopy (^{1}H NMR) in a 250 MHz Avance DPX 250 Bruker instrument. Raman (Renishaw system 3000) and Fourier transform infrared FT-IR (Perkin-Elmer Spectrum) spectroscopies were used to monitor the number of double bonds before and after cross-linking and etching of the PI−PDMS.

Rheology. Rheological measurements were used to determine the order−disorder transition temperature (T_{ODT}) of the synthesized polymers. The viscoelastic properties of the diblock copolymers were investigated by isothermal and temperature-gradient dynamic mechanical measurements on a Rheometrics RS 800 rheometer using parallel plate geometry. The temperature was changed continuously with a rate of 2.5 °C/min.

Electron Microscopy. Samples were investigated in a Jeol 3000F transmission electron microscope (TEM). Preparation for microscopy was performed by placing a piece of the sample in an Agat mortar filled with liquid nitrogen and crushed into a fine powder. Then the mortar was filled with ∼2 mL of toluene (Fluka, 99.8% pure), and the suspension was transported to a small glass. The glass with suspension was placed in an ultrasonic water bath (Branson, Model B1510-MT) for 30 min to separate particles. A drop of the suspension was deposited on a holey carbon film on a 300 mesh copper grid. Finally, the toluene was evaporated and the sample analyzed by TEM.

SAXS. Small-angle X-ray scattering (SAXS) was performed using the rotating anode lab source at Risø DTU. The wavelength of the X-rays was $\lambda = 1.54$ Å. A two-dimensional position-sensitive wire detector in a distance of 1435 mm from the sample was used to collect scattered radiation.

SANS. Samples were investigated using the small-angle neutron scattering instrument SANS-II at SINQ, Paul Scherrer Institute (PSI) in Villigen, Switzerland,[19] using 6 m collimation with entrance and exit pinholes equal to 16 and 6 mm, respectively. The sample-to-detector distance was 6 m, and the neutron wavelength was 6.37 Å.

Samples were placed in glass cuvettes. In case of the swelling experiments the cuvettes were filled with ∼2 mL of solvent just before placing in the sample chamber and starting scattering measurement. During the swelling process time-resolved scattering data were collected over 60 or 300 s intervals. Some samples were measured for longer time when necessary (1200 or 3600 s).

Results and Discussion

First, we present data on the precursor diblock copolymer and the samples derived from this, which result from following the prescribed procedure. Second, we show the results of a more detailed study using SANS. The SANS measurements gauge the structural response of the samples to various solvents and shed light on the morphological identity of the collapsed samples.

Characteristics of Precursors and Cross-Linked, Etched Material. *Block Copolymer Parent Sample*. A PI−PDMS

block copolymer (ID33) was synthesized by anionic "living" polymerization as described above. Table 1 lists the characteristics of the precursor diblock copolymer. SEC and/or ^{1}H NMR were applied in order to obtain the molecular weights of the PI block, the total weight of the block copolymer, the polydispersity index, and the weight and volume fraction of PDMS. SAXS measurements showed that the morphology of the parent sample is hexagonally (HEX) ordered cylinders of PDMS in a matrix of PI. Rheological studies determined the order−disorder temperature (T_{ODT}).

Preparation of Samples by Cross-Linking and Etching. Generally, our experience is that effective cross-linking of PI requires several treatments with peroxide. Previously, we have reported that five to six additions of fresh peroxide was necessary to obtain sufficient mechanical stability of the PI network after etching with HF.[14] Figure 1 presents the expected mechanism of cross-linking the PI chains.[22] High temperature causes the dicumyl peroxide molecule to split into two radicals. These radicals attack the allylic hydrogen in PI, and new radicals are created within the chain. When two radicals on different chains react with each other, a cross-link is created, without changing the double bond which is untouched by this reaction. One peroxide molecule generates on average one (or less) cross-link. At high temperature and high cross-linking degrees the double bonds can take part in additional cross-linking.

TBAF etching procedure was previously used by others.[23] The mass loss due to etching is a first good indication of rendering a nanoporous material if it approaches the sample mass of PDMS. Fractions of mass losses following the etching procedure were respectively 0.26 and 0.23 for ID33-x14e and ID33-x20e. The data show good agreement between the fraction of mass loss and the original weight fraction of PDMS (w_{PDMS}) listed in Table 1. This supports the conclusion that the PDMS block was quantitatively removed. Sample ID33-x20e shows a slight deficit in this comparison, which may mean that the removal of PDMS is not perfect in this particular sample.

Structural Results. Following the preparation of cross-linking and etching described above, the samples were characterized by both SAXS experiments and microscopy. Structural data for the dry samples (which are not exposed to any form of solvent) are presented in Table 2.

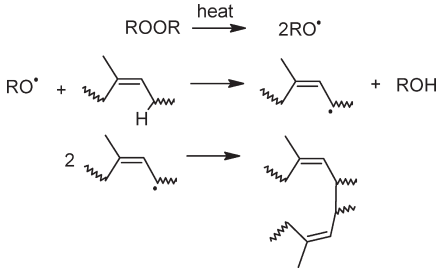

Figure 1. Scheme for cross-linking of PI by thermal treatment with a peroxide.

Figure 2 shows azimuthally reduced SAXS data representing the three steps of preparing a sample from the precursor polymer: the mother (original) sample (ID33), the cross-linked sample (ID33-x20), and the cross-linked and etched sample (ID33-x20e). In case of the precursor polymer the scattering gives evidence to a hexagonal structure by the presence of the higher order peaks at ratios of $\sqrt{3}$ and $\sqrt{7}$ with respect to the primary scattering peak q^*. After cross-linking the higher order scattering peaks have vanished, but an intense primary peak remains, which very likely is Bragg scattering from the ordered structure which is still present in the sample. The peak position is shifted to little higher q values, which is indicative of a slight shrinkage. Although a natural consequence of the selective etching is an increase of contrast between the cavity voids and the PI matrix compared to the contrast between PDMS and PI, the ID33-x20e sample gives no nanoporous scattering profile following the preparatory steps as observed in other samples.[24] The absence of any indication of a nanoporous structure for the collapsed sample is similar to previous observations.[13]

In the inset in Figure 2 a position on the q scale is marked, which is calculated assuming that the volume of the cross-linked PI matrix (a soft elastomer) does not change or is influenced in any way during selective etching of the PDMS minority component. As etching progresses, the cylindrical

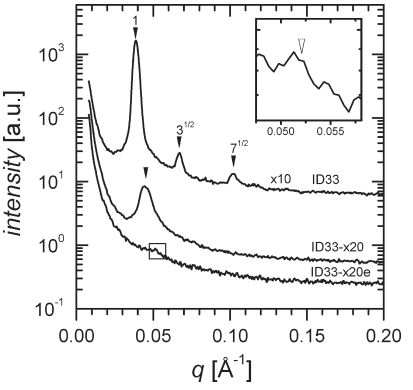

Figure 2. Azimuthally averaged SAXS data of the original precursor (ID33), the cross-linked (ID22-x20), and the etched (ID33-x20e) samples. In order to separate plots for better presentation, the top scattering profile is multiplied by a factor of 10. The primary peak position (q^*) is marked by numeral "1" and higher order reflections are marked accordingly showing the indications of a hexagonal structure. The inset in the top right corner magnifies the scattering curve for sample ID33-x20e in the vicinity of the 0.05 Å^{-1} scattering vector. The open triangle indicates the maximum expected peak position for a vanishing nanoporous structure (see text). The weak peak at 0.051 Å^{-1} hints the presence of a slight contrast (change of PI density) at the centers of the collapsed cylindrical cavities.

Table 2. Structural Data for Dry Samples (without Exposure to Solvents) and Wet Samples[a]

	dry					wet (in d-toluene)	
	precursor	cross-linked		etched		etched	
sample codes	ID33	ID33-x14	ID33-x20	ID33-x14e	ID33-x20e	ID33-x14e	ID33-x20e
SAXS q_{10} [Å^{-1}]	0.0387	0.0452	0.0448	0.0489[b]	0.0513[b]		
$2\pi/q_{10} = d_{10}$ [Å]	162	139	140	128	122		
SANS q_{10} [Å^{-1}]		0.0426	0.0426	no peak	no peak	0.0374	0.0400
$2\pi/q_{10} = d_{10}$ [Å]		147	147			168	157

[a] The results of Bragg spacing (d_{10}) measurements are listed for SAXS and SANS experiments. Data accuracy for SAXS and SANS is about 1% and 5%, respectively. [b] This is an observation of a very weak "bump" in the q-position, which indicates the maximum q-value possible given conditions discussed in the text.

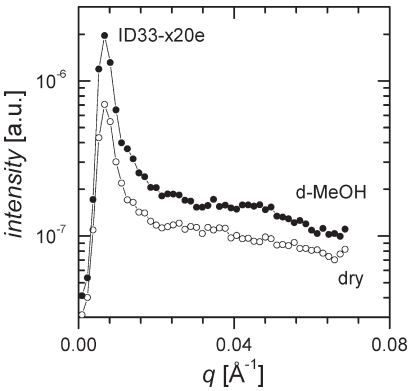

Figure 3. Azimuthally averaged SANS profiles of the raw scattered intensity of sample ID33-x20e. Scattering from the sample in the dry state is depicted by open symbols, and scattering from the sample placed in d-methanol is depicted by closed symbols. The high intensity at very low q is parasitic scattering due collimation of the neutron beam and background intensity.

PDMS domains reduce in size and cause a shrinking of the hexagonal structure. As the etching is complete the cylindrical domains have totally collapsed, all PDMS is removed, and there is no longer any scattering contrast in the polymer. A position on the q scale can be calculated based on the peak position of the cross-linked polymer prior to etching, which is equivalent to the highest possible q value of scattering from the etched collapsed system. The very small peak at 0.051 $Å^{-1}$ can be interpreted as due to small PI density modulation at the centers of the collapsed cylindrical domains.

Attempts of obtaining electron micrographs of the nanostructure in samples ID33-x14e and ID33-x20e were conducted in vain. From this evidence we conclude that there are no nanopores in the as-prepared dry samples from the batch of ID33.

SANS Investigation of Morphology Responses to Selected Solvents. Before investigating sample response to various solvents, we present the SANS profiles of the dry sample ID33-x20e in Figure 3 (open symbols). The SANS data show an absence of any constructive Bragg scattering for ID33-x20e, which is in agreement with the collapsed state, as discussed in the previous section.

In the following sections we will investigate how the sample behaves when exposed to respectively a nonsolvent and a solvent for the cross-linked PI matrix. We do this in the hope that such investigation can shed light on the nature of the unresolved structure of the collapsed material. The question is whether a nonsolvent will percolate into the PI matrix by reopening the original nanocavities. When using a deuterated liquid, the contrast factor between filled cavity and matrix will be greatly enhanced and in this way amplify otherwise weak Bragg scattering. On the other hand, the expectation for a solvent is that the sample will undergo swelling and that the matrix will change dimensions.

Exposure to a Nonsolvent (Methanol). Methanol is a nonsolvent for the cross-linked PI matrix. The exposure of the ID33-x20e sample to deuterated methanol did not yield any change of the scattering as judging from the SANS profile in Figure 3 (closed symbols). The scattering remains indecisive and does not characterize the morphology of the sample beyond the level of being collapsed in agreement with the dry SANS and SAXS data. The data indicates that there is no trace of the original structure left in the sample, which could facilitate a guided percolation of the nonsolvent.

Exposure to a Solvent (Toluene). Toluene is a solvent for the cross-linked PI matrix. The second liquid exposure

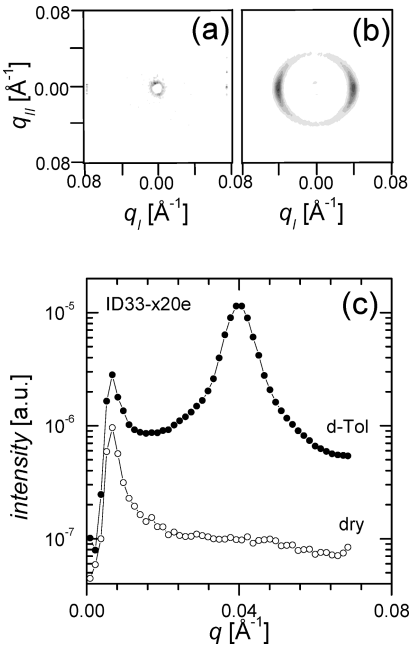

Figure 4. Two-dimentional scattering patterns recorded for the sample ID33-x20e in (a) the dry state without any solvent exposure and (b) in the wet state where the same sample was placed in d-toluene for 150 min. SANS data were collected for 300 s in both cases. The azimuthally averaged data are compared in (c).

experiment is an attempt to swell the complete sample matrix and study the effect of this on the sample structure. Placing the sample in toluene will cause swelling of the cross-linked matrix.

As illustrated in Figure 4, this led to a dramatic change of the scattering fingerprint of the collapsed sample ID33-x20e. The two-dimensional detector response shows the scattering collected over 300 s. Figure 4a shows the scattering from the dry sample. After being submerged in deuterated toluene for 2.5 h a very strong scattering signal is observed as illustrated in Figure 4b. Obviously, the solvent swells the sample and apparently fills out the empty pore cavities. The two-dimensional scattering is anisotropic, which is in perfect agreement with the extrusion processing during sample preparation. Hence, the sample holds a memory of both the originally templated diblock morphology and the preparation alignment procedure, which persists matrix cross-linking and nanoporous etching. At the end of the preparation procedure the dry sample renders no structure, but when the cross-linked matrix is swollen by a solvent, the nanostructured morphology makes its presence. The azimuthally integrated scattering pattern in Figure 4c allows a precise identification of the Bragg peak position. The scattering peak positions of the swollen ID33-x14e and ID33-x20e samples are relatively close to each other (as seen in Table 2) and in good agreement with the preparatory procedure which suggest that the higher cross-linked sample exhibits the smaller Bragg spacing of the swollen polymer and vice versa.

Swelling Kinetics of Collapsed Structure. Finally, we want to test how well a collapsed sample will reproduce the behavior of exhibiting nanoporous structure during swelling. In order to do this, the sample ID33-x14e was subjected to repetitive cycles of swelling in d-toluene followed by drying in air. This was done online in the SANS instrument and enabled investigation of the kinetics of the swelling as well as the reproducibility of cycles of swelling and drying.

Figure 5 shows the time evolution of two swelling−drying cycles. The azimuthally averaged SANS profiles of scattering

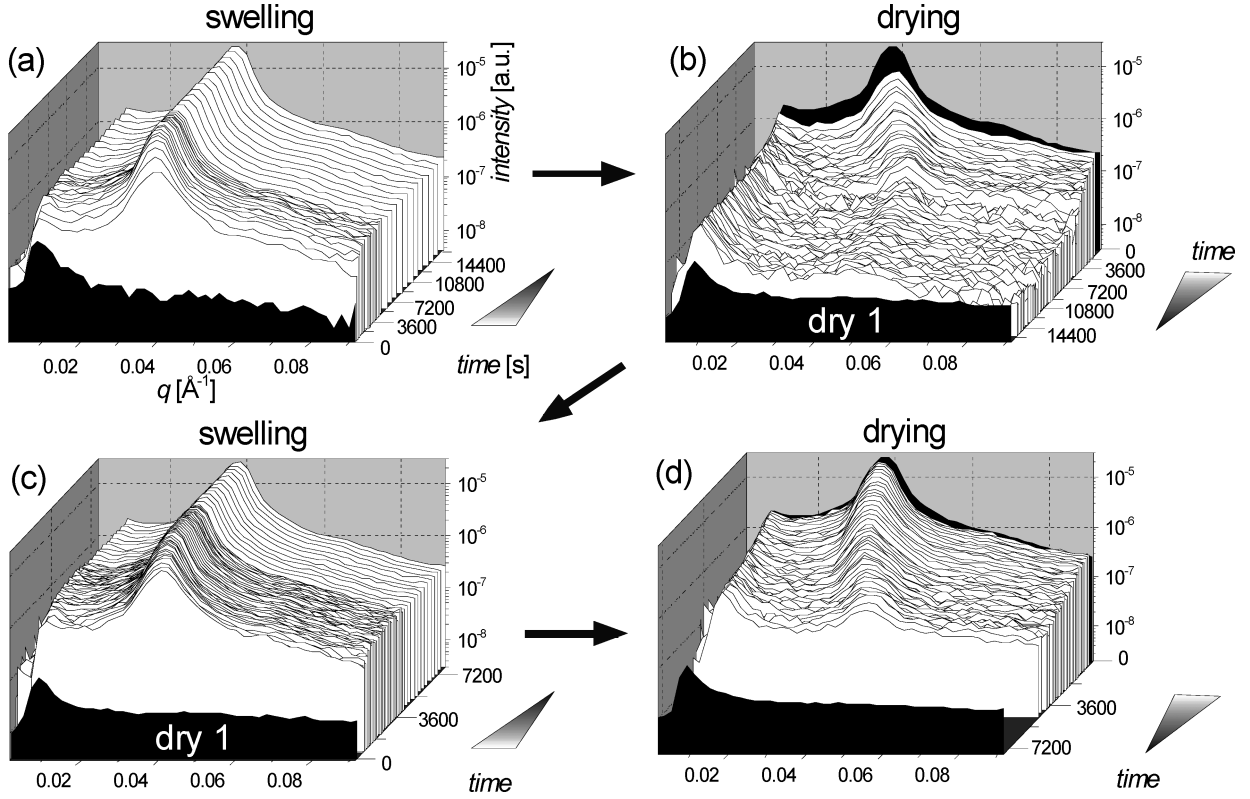

Figure 5. Time evolution of repeated swelling and drying as observed in the azimuthally averaged SANS profiles. The initial and resulting dry states are shown at the front of each sequence of data which shows the scattering intensity versus scattering vector q. The sample ID33-x14e was exposed to (a) swelling, (b) drying, (c) repeated swelling, and (d) repeated drying. Notice the direction of the time axis is alternatively reversed for clarity of the evolution of the scattering profiles.

intensity versus scattering vector q show evidence of the structural changes in the sample. The scattering from the dry state of the sample is indicated in black at the front of Figure 5a. There is no scattering peak from nanostructure in the dry sample. After submerging the sample into d-toluene the first 60 s frame of scattering was recorded with a time delay of 4.5 min. This is due to the handling procedure of introducing the solvent and the safety routine for the neutron exposure. A scattering peak is clearly evident at this time, and the scattering vector q^* at peak intensity maximum decreases following time, in agreement with an increase of the real space dimensions of the material structure.

Figure 5b presents the scattering recorded during sample drying. The last recorded wet scattering profile from the swelling is put at the back of this series of profiles for comparison and marked in black. As anticipated, the peak position at maximum intensity increases and the intensity drops over time. After 4 h the scattering peak is almost gone. Following subsequent drying of the sample in air for 6 h and another 2 h in a vacuum chamber the resulting scattering marked "dry 1" is displayed as the black plot at the front. This scattering gives proof that the swelling-induced nanostructure (in the form of a peak of intensity) has completely gone. Back at the starting point the sample was exposed to a second swelling experiment, and the resulting evolution on the scattering is documented in Figure 5c. The effect of the d-toluene solvent is identical to the first cycle. Finally, the sample was dried for the second time as illustrated in Figure 5d. The evolution in the scattering does not completely reproduce the evolution of the first drying sequel. Drying conditions were not subjected to particular control, and the two drying experiments are not comparable in a detail that justifies a close relative inspection of the two cycles. However, the scattering data of the swelling behavior are a more precise intrinsic measurement of the interaction between solvent and sample, and the repeated swelling sequences will be the subject of work to follow and future publications.

A fully dried sample was obtained after 3 h, which shows no nanostructured scattering. Hence, we can conclude that the two swelling−drying cycles resulted in repeated appearance and disappearance of the nanostructure. We interpret this as being in fact an opening and closing of nanoporous voids, which are templated into the collapsed sample by the original morphology of the diblock precursor polymer ID33. Also, the sample reproduced the originally introduced alignment by the shear extrusion preparation process as evidenced by the 2D scattering profile, which shows strong equatorial peaks similar to those of Figure 4b. In conclusion, this set of data shows that the collapsed material exhibits memory of the sample history on two accounts, namely precursor morphology and preparatory alignment.

Conclusions

We have examined the structure and behavior of a collapsed elastomeric PI-matrix material which was prepared from diblock copolymer precursors by cross-linking and selective etching of the minority block. At first sight the sample displayed no structural evidence as investigated by TEM, SAXS, and SANS measurements of dry specimens. However, this cross-linked material exhibited interesting properties as a gel when exposed to solvent which swells the PI matrix. A nanostructure is dormant and recovers inside the gel in such a fashion that the anticipated porosity is re-established, which matches the nanostructure of the precursor block copolymer material. The appearance of structure seems to be driven by a process, which swells the matrix and

inflates the cavities, which are vacated by the original expendable block copolymer component. These results resemble observations by Durkee et al. in a study on the microstructure in cross-linked diblock copolymer gels, which reported on solvent-filled open channels inside a network of swollen PI.[27] Furthermore, the structure also exhibits perfect agreement with the process of extrusion that was part of the preparation procedure. This was evidenced by anisotropic scattering caused by the presence of elongated (solvent filled) cavity structures aligned in the extrusion direction. Hence, the collapsed elastomeric material has memory of the original precursor morphology and the preparatory extrusion alignment. Upon cycles of swelling and drying the nanostructure shows up and disappears—reversibly, which suggests that the presence and absence of solvent can open and close the cavities. Very interestingly, the cavities are not prone to be opened by nonsolvents to the matrix, which suggests that the nature of the liquid (solvent or nonsolvent) could control the state of the material in e.g. a membrane application. This means that the material could have some "smart" application in advanced separation systems and maybe used as a form of valve, where the liquid polarity would be the controlling external stimuli.

Acknowledgment. This work was supported by a grants given by the Danish Research Council for Technology and Production Sciences (FTP Grant 26-03-0271), DANSCATT centre sponsored by the Danish Natural Science Research Council. The authors thank Thomas Geue at the Paul Scherrer Institute (Villingen, Switzerland) for providing beam time at the SANS 2 instrument, Pia Wahlberg at the Danish Technological Institute (Høje Taastrup, Denmark), for help with SEM and Fengxiao Guo at the Department of Chemical Engineering, DTU (Kgs. Lyngby, Denmark), for sample preparation. M.E.V. is grateful for support given by Kaj Hansen's Foundation (Danalim Prisen).

References and Notes

(1) Wei, Z. G.; Sandstrom, R.; Miyazaki, S. *J. Mater. Sci.* **1998**, *33*, 3743–3762.
(2) Pei, Q. B.; Inganas, O. *Adv. Mater.* **1992**, *4*, 277–278.
(3) Gazotti, W. A.; Casalbore-Miceli, G.; Geri, A.; Berlin, A.; De Paoli, M. A. *Adv. Mater.* **1998**, *10*, 1522.
(4) Koberstein, J. T.; Duch, D. E.; Hu, W.; Lenk, T. J.; Bhatia, R.; Brown, H. R.; Lingelser, J. P.; Gallot, Y. *J. Adhes.* **1998**, *66*, 229–249.
(5) Gil, E. S.; Hudson, S. A. *Prog. Polym. Sci.* **2004**, *29*, 1173–1222.
(6) Baughman, R. H. *Synth. Met.* **1996**, *78*, 339–353.
(7) Harmon, M. E.; Tang, M.; Frank, C. W. *Polymer* **2003**, *44*, 4547–4556.
(8) Mortensen, K.; Pedersen, J. S. *Macromolecules* **1993**, *26*, 805–812.
(9) Mortensen, K.; Almdal, K.; Kleppinger, R.; Mischenko, N.; Reynaers, H. *Physica B* **1997**, *241*, 1025–1028.
(10) Yerushalmi, R.; Scherz, A.; van der Boom, M. E.; Kraatz, H. B. *J. Mater. Chem.* **2005**, *15*, 4480–4487.
(11) Olson, D. A.; Chen, L.; Hillmyer, M. A. *Chem. Mater.* **2008**, *20*, 869–890.
(12) Hillmyer, M. A. *Adv. Polym. Sci.* **2005**, *190*, 137–181.
(13) Guo, F.; Andreasen, J. W.; Vigild, M. E.; Ndoni, S. *Macromolecules* **2007**, *40*, 3669–3675.
(14) Hansen, M. S.; Vigild, M. E.; Berg, R. H.; Ndoni, S. *Polym. Bull.* **2004**, *51*, 403–409.
(15) Ndoni, S.; Vigild, M. E.; Berg, R. H. *J. Am. Chem. Soc.* **2003**, *125*, 13366–13367.
(16) Guo, F.; Jankova, K.; Vigild, M. E.; Ndoni, S. *Polym. Prepr.* **2008**, *49*, 540.
(17) Ndoni, S.; Papadakis, C. M.; Almdal, K.; Bates, F. S. *Rev. Sci. Instrum.* **1995**, *66*, 1090–1095.
(18) Andersen, K.; Diplom, K. Thesis, Dept. of Chemical Engineering, Technical University of Denmark, Lyngby, Denmark, **2005**.
(19) Strunz, P.; Mortensen, K.; Janssen, S. *Physica B* **2004**, *350*, e783–e786.
(20) Mark, J. E., Ed. *Polymer Data Handbook*; Oxford University Press: New York, 1999.
(21) Brandrup, J.; Immergut, E. H. *Polymer Handbook*, 3rd ed.; John Wiley & Sons: New York, 1989.
(22) Krevelen, V. D. W., Ed. *Properties of Polymers*; Elsevier: Amsterdam, 1990.
(23) Cavicchi, K. A.; Zalusky, A. S.; Hillmyer, M. A.; Lodge, T. P. *Macromol. Rapid Commun.* **2004**, *25*, 704–709.
(24) Ndoni, S.; Vigild, M. E.; Berg, R. H. *J. Am. Chem. Soc.* **2003**, *125*, 13366–13367.
(25) Higgins, J. S.; Benoît, H. C. *Polymers and Neutrons Scattering*; Oxford University Press: New York, 1997.
(26) Li, Y.; Tanaka, T. *J. Chem. Phys.* **1990**, *92*, 1365–1371.
(27) Durkee, D. A.; Gomez, E. D.; Ellsworth, M. W.; Bell, A. T.; Balsara, N. P. *Macromolecules* **2007**, *40*, 5103–5110.